

A Tubular Network Assembled from Silver Nanoparticles

Guangqing Yan,^[a] Li Wang,^{*[a]} Haojie Yu,^[a] Lei Zhang,^[a] Jingmin Gao,^[a] Jianjun Wang,^[a] Liang Ma,^[a] Yulai Zhao,^[a] Qian Wu,^[a] and Abid Muhammad Amin^[a]

Keywords: Silver / Nanotubes / Nanoparticles / Tubular network / Conducting materials / Micelles

A novel submicron-sized tubular network composed of rolled silver nanosheets was successfully fabricated by the assemblage of silver nanoparticles in a reverse micellar solution; the size of these assembled nanoparticles was ca. 3 nm and they had a narrow size distribution. The molar ratio between H₂O and lauric acid in the reaction media was found to significantly effect the structure of the resultant tubular network.

This study further showed that these nanostructures are stabilized by lauric acid, which contributed to the assemblage of the network. After detailed analysis, a possible reaction mechanism was determined, and these nanostructures showed obvious advantages and potential application as conductive fillers in coatings, especially because of their unique network morphology.

Introduction

It is well known that conductive coatings have wide application in our daily life, and they are primarily composed of two components: a polymeric matrix and a conductive filler. The conductivity of these coatings is predominantly determined by the type of metal filler employed, which is usually nickel,^[1,2] copper,^[3,4] silver^[5–7] or an alloy of these metals. Owing to its high conductivity and stability, silver is considered as an excellent and promising metal filler candidate, but there are still plenty of aspects related to the use of silver that need to be improved. Ordinarily, a high silver filler content is needed to achieve high coating conductivity, but this will inevitably impair the performance of the polymeric matrix.^[8] Therefore it is necessary to determine an effective route to obtain high conductivity, while keeping the silver content of the composite coating low. One of the most feasible and effective ways to achieve this goal is to introduce silver nanomaterials into the conductive filler, and in this way the total silver content of the coating is reduced, while still maintaining good conductivity by coating film.^[9,10] Currently, silver nanowires are considered to be the ideal nanostructures for improving the conductivity of coatings because of their 1D morphology. Moreover, a number of different synthetic routes have been developed for the fabrication of silver nanowires, although the soft solution method is primarily considered to be the most popular and effective synthetic strategy.^[11–14] However to date, the simple and rapid production of silver nanowires is still infeasible. The improvement of this method, or the

development of alternative means of preparation, for wide application is urgently required.

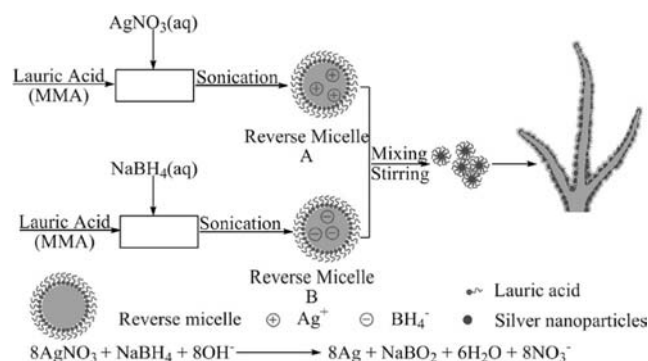
We have successfully obtained a group of novel nanotubular networks, which have been built by the assemblage of silver nanoparticles in a reverse micellar solution. These networks are connected by rolled nanosheets rather than seamless nanotubes. However, these nanostructures would be favorable candidates for improving silver-doped conductive coatings because of their morphologies and small sizes. It has been reported that these silver nano-assemblies could transform into continuous silver nanostructures after being sintered at high temperatures.^[15] Therefore, it is feasible for these nanoassemblies to become conductive after a similar treatment. We found that the width of the rolled nanosheets was about 500 nm, and the diameter of the nanoparticles from which they were assembled were only 3 ± 1 nm. Lauric acid played a very important role in this assembly procedure. The hydrophobicity of this acid, and the resultant steric repulsion between different assembled silver nanoparticles is considered to be the main influence on the self-assembly process. In principle, the morphology of the nanosheets is advantageous for the formation of a conductive network in a polymeric matrix, and such a tubular silver network could be ideal as a conductive filler in coatings, after further treatment. Furthermore, the synthetic process for the generation of these nanostructures is relatively reproducible, highly efficient and facile. Accordingly, the synthesis of these silver nanotubular networks is promising and of significance.

Results and Discussion

In this study we fabricated a group of novel silver nanotubular networks using a water-in-oil reverse micellar system. In this system, lauric acid was exploited as the surfac-

[a] State Key Laboratory of Chemical Engineering, Department of Chemical and Biological Engineering, Zhejiang University, Hangzhou 310027, People's Republic of China
Fax: +86-571-8795-1612
E-mail: opl_wl@dial.zju.edu.cn

tant to form the reverse micelles, and methyl methacrylate (MMA) was used as the organic phase, as shown in Scheme 1. Previously, Liu et al. reported that individual silver nanotubes could be synthesized in a reverse micellar solution with octanoic acid as the surfactant.^[15] In their report, these authors proposed that acid would form reverse micelles after adding an aqueous solution of it to MMA, and then different micelles (A and B in Scheme 1) would further collide with each other to generate silver nanoparticles that are stabilized by the surfactant. These nanoparticles would assemble into nanotubes that would be directed by the behavior of the hydrophobic part of the surfactant cluster in the organic phase. In contrast to Liu et al.'s work, we have adopted lauric acid in our study, and instead of the 1D nanotubes formed in the octanoic acid solution, rolled nanosheet assemblies were predominately formed in the lauric acid solution. Most interestingly, the network morphology is very favorable for the formation of conductive networks and meaningful for the improvement of conductive coatings.^[15] Figure 1 shows the silver tubular networks we prepared following the standard procedure shown in Scheme 1. From the high resolution TEM image, we can see that the network is assembled from numerous nanoparticles with a diameter of 3 ± 1 nm. Due to their small size these nanoparticles appeared to be of poor crystallinity, furthermore the spacing between the assembled nanoparticles was commonly less than 3 nm. In addition, the EDX spectrum (Figure 1) of the sample indicated that elemental silver existed in these nanostructures, and the C:O molar ratio was 5.6:1, which is similar to the value in lauric acid (6:1).



Scheme 1. Typical procedure of the lauric acid assisted reverse micellar method for the fabrication of silver nanotubular network.

The minor difference between these values may be due to the influence of the ambient C and O. The molar ratio between Ag and lauric acid was 1.53:1, which showed that these silver nanoparticles had a large fraction of surface atoms. Liu et al.^[15] reported that in their nanostructures were formed by the assemblage of the silver nanoparticles. From the SEM image, we can see that in our case the network is formed from rolled nanosheets, and not planar nanosheets or seamless nanotubes. These assembled silver nanoparticles have a small size and the bonding between the silver atoms and carboxyl groups of the lauric acid is not as strong as the bonding between Ag and thiol groups,

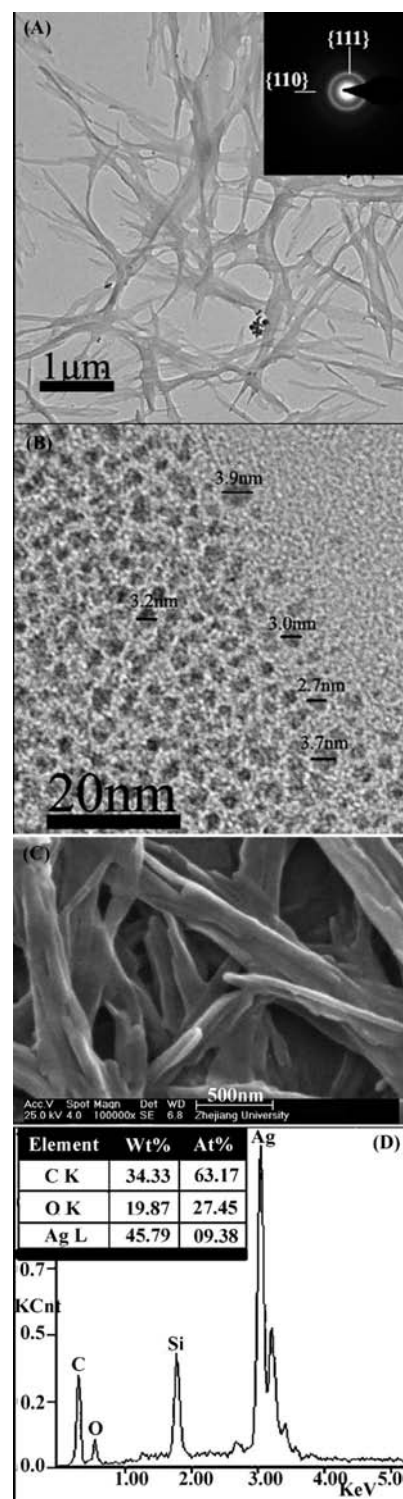


Figure 1. TEM (A) and HRTEM (B) images of tubular silver networks prepared following the standard procedure detailed herein. The inset in (A) is the selected angle electron diffraction (SAED) pattern for the silver nanoassembly recorded by directing the electron beam perpendicular to the plane we observed without tilt. Image (C) is the SEM image of the silver networks. Figure (D) shows the spectrum and results of energy dispersive X-ray analysis (EDX) of the networks.

Ag and amino groups, etc; therefore, the carboxyl-bonded silver nanoparticles are expected to have a higher activity

than these other groups, and the carboxylic surfactants can be easily removed or substituted. Such nanostructures might attract attention in many fields such as fluorescence,^[16,17] catalyst,^[18,19] and Surface-Enhanced Raman Scattering (SERS).^[20,21]

The lauric acid-assisted reverse micellar method for the fabrication of silver nanotubular networks. To study the reproducibility of our method, and to evaluate other influencing factors, parallel experiments with different water/acid molar ratios (W values) were performed. As shown in Table 1, experiments 1–5 were carried out at $W = 20, 40, 80$ by two different methods: (i) the W value was adjusted by changing the amounts of the precursors added to the reaction solution; (ii) the W value was adjusted by altering the concentration of the surfactant, lauric acid, in the solution. From Figure 2 we can see that the nanostructures, which form by the assemblage of silver nanoparticles, were all generated under different conditions and the diameters of the majority of assembled nanoparticles displayed no obvious change when the reaction conditions were altered. It is evident that this preparation method is highly reproducible and stable. However, there were some slight morphological changes to the product nanostructures when the reaction conditions were altered. The network fabricated at when $W = 80$ was decorated by some large silver nanoparticles on the outer surface of the nanostructure, and they (Figure 2, image D) were much more densely decorated by large nanoparticles with a diameter of ca. 10 nm. We suggest that the nonuniformity of the products from these two reactions resulted from the weakened protection of the nanoparticles due to the reduction in the amount of lauric acid and the increase in the amount of silver precursor used in the latter experiment. Experiments with low W values gave silver nano-assemblies that were preferentially organized into individual nanotubes with few branches and regular surfaces. Experiments with high W values produced assemblies that were tight tubular networks with many branches and irregular surfaces.

Table 1. Synthesis of the silver nanotubular networks by the assistance of lauric acid.

Run	AgNO ₃ (aq.)		NaBH ₄ (aq.)		Lauric acid/ MMA		$W^{[c]}$
	V [μL]	C [M]	C [μL]	C [M]	$V^{[a]}$ [mL]	$C^{[b]}$ [M]	
1	144	0.2	144	0.2	5	0.04	40
2	72	0.2	72	0.2	5	0.04	20
3	288	0.2	288	0.2	5	0.04	80
4	144	0.2	144	0.2	5	0.08	20
5	144	0.2	144	0.2	5	0.02	80

[a] V : volume of the MMA/carboxylic acid solution. [b] C : concentration of carboxylic acid in the solution. [c] W : molar ratio between H₂O (from the added aqueous solutions of AgNO₃ and NaBH₄) and the added carboxylic acid; the experiments (runs 1–5) were all performed at room temperature (ca. 30 °C).

It was assumed that the self-assembly of silver nanoparticles into tubular networks was due to the intermolecular action of the hydrophobic part of the surfactants.^[15] Fig-

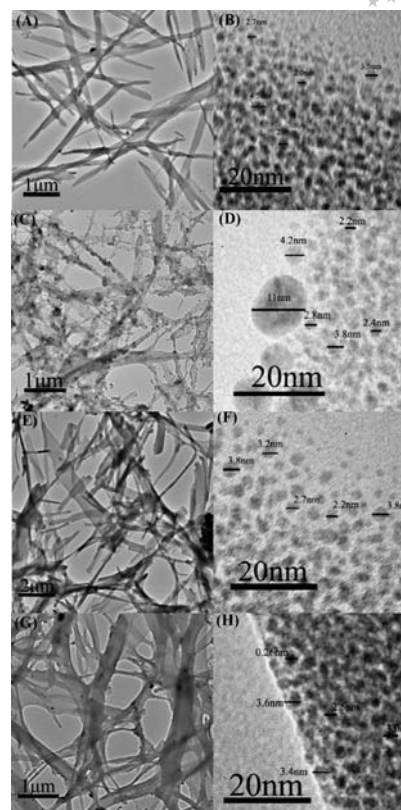


Figure 2. TEM and HRTEM (inset) images of the silver nanotubular networks synthesized at various W values that were adjusted by different routes. (A) and (B) $W = 20$, adjusted by changing the amount of H₂O in the AgNO₃ and NaBH₄ aqueous solutions, respectively; (C) and (D) $W = 80$, adjusted by changing the amount of H₂O in the AgNO₃ and NaBH₄ aqueous solutions, respectively; (E) and (F) $W = 20$, adjusted by changing the concentration of lauric acid; (G) and (H) $W = 80$, adjusted by changing the concentration of lauric acid.

ure 3 shows the IR spectra for lauric acid and the silver nano-assembly formed in run 1 (Table 1). The major difference in these spectra is that the strong adsorption peak of lauric acid located at 1696.1 cm⁻¹ in its spectrum is blue-shifted to 1561.1 cm⁻¹ in the spectrum of tubular silver network. However, the spectra of both lauric acid and the silver nano-assembly show the following characteristic absorption peaks: $\delta_{C-H} = 1464$ and 1407 cm⁻¹, $\gamma_{C-H} = 723$ cm⁻¹ corresponding to (–CH₂–)₁₀. As the peak at 723 cm⁻¹ is only observed for (–CH₂–)_{*n*} groups with $n > 4$, its presence in the spectrum of the silver nano-assembly indicates that the long carbon chain of lauric acid is present in this sample. Furthermore, there are two characteristic –COOH group absorption peaks in the IR spectrum of lauric acid, $\nu_{C=O} = 1703$ and $\nu_{C-O} = 1294$ cm⁻¹ (Figure 3), that have disappeared or are shifted in the IR spectrum of the silver nano-assembly. Additionally, the spectrum of the silver nano-assembly shows a peak located at 1561 cm⁻¹. It has been reported that Ag^I can coordinated with L-histidine and (S)-(–)-2-oxopyrrolidine-5-carboxylic acid through –COO–Ag bonds,^[22] and that the surface atoms of silver nanowires can coordinated with polyvinyl pyrrolidone

(PVP) through the interaction between carbonyl and silver atoms.^[23,24] In addition, oleate has been used to fabricate silver colloids, the IR spectrum of which displayed similar changes when compared to the spectrum of oleic acid that we observe when comparing the spectra of our silver nano-assemblies and lauric acid.^[25] However, the details of the binding mode between carboxyl and silver atoms is still not clearly understood in this situation. After extensive analysis, we are in a position to propose one possible binding mode: that both the oxygen atoms in the lauric acid carboxyl group coordinate with a surface silver atom of the nano-structure. This mode satisfies the requirements of bond valence, and is also consistent with the phenomenon observed in IR spectra i.e. only one vibrational adsorption peak is located between the $\nu_{\text{C=O}}$ and $\nu_{\text{C-O}}$ peaks.

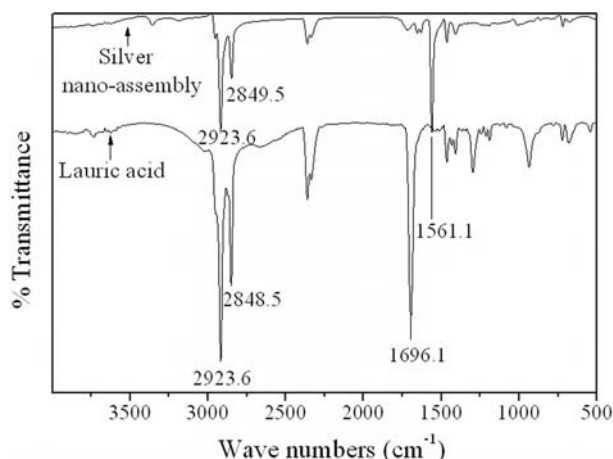


Figure 3. FT-IR spectra of lauric acid and the silver nanotubular network. Lauric acid: $\nu_{\text{C-H}} = 2924 \text{ cm}^{-1}$, $\nu_{\text{C-H}} = 2954 \text{ cm}^{-1}$, $\nu_{\text{C=O}} = 1703 \text{ cm}^{-1}$, $\delta_{\text{C-H}} = 1464 \text{ cm}^{-1}$, $\nu_{\text{C-O}} = 1294 \text{ cm}^{-1}$, $\gamma_{\text{C-H}} = 723 \text{ cm}^{-1}$; silver nano-assembly: $\nu_{\text{C-H}} = 2923 \text{ cm}^{-1}$, $\nu_{\text{C-H}} = 2923 \text{ cm}^{-1}$, $\nu_{\text{C-O}} = 1561 \text{ cm}^{-1}$, $\delta_{\text{C-H}} = 1464 \text{ cm}^{-1}$ (1407 cm^{-1}), $\gamma_{\text{C-H}} = 723 \text{ cm}^{-1}$.

There are some adsorption peaks of moderate intensity in the IR spectrum of lauric acid that are absent from the spectrum of the silver nano-assemblies. The absence of these peaks from the nano-assembly spectrum can be explained by the dissociation of lauric acid into the anion after adsorption onto the surface of the silver nanoparticles. In conclusion, the stability and assemblage of these silver nanoparticles was due to the intermolecular action of the adsorbing lauric acid.

It has been reported that the amphiphilicity of a surfactant influences the manner in which it self-assembles.^[26] Therefore tuning the amphiphilicity of surfactants can be used to fabricate different silver nano-assemblies. The interparticle forces for nanoscale self-assembly commonly include van der Waals, magnetic, molecular or entropic forces.^[27] In this system, van der Waals and entropic forces (steric repulsion, electrostatic force etc) are the main effects in the self-assembly process; van der Waals forces are present between any two material bodies, and usually act in as an attractive force to bring nanoparticles together. The adsorbed carboxylic acid also provides some affinity due to

the hydrophobicity of its long hydrocarbon chain. Conversely, the electrostatic force and steric repulsion provide the repulsive forces for the self-assembly and protect the nanoparticles from aggregating into a bulk state. These two kinds of opposing forces need to be balanced, and the nano-assemblies need to stay in the lowest energy state. Different carboxylic acids provide different levels of affinity and repulsion, and therefore result in different lowest energy states for the nano-assemblies.^[28] However, the detailed mechanism as to how the tubular network is formed is still unknown and needs further investigation. What is known is that stabilizing ligands and appropriate solvent are indispensable for the self-assembly process or else the nanoparticles would precipitate from solution. The steric repulsion generated by lauric acid adsorbed on the nanoparticle's surface is dependent on the length and adsorption density of this surfactant. If insufficiency lauric acid is present it is inevitable that the silver nanoparticles that are generated would agglomerate into large particles to compensate for the weakened steric repulsion provided by the surfactant molecules. As shown in Figure 2, image D, these large particles then further self-assemble epitaxially onto the outer surface of the nanotubular network to form large particle decorated nano-assemblies.

As mentioned before, the nanotubular networks do not comprise seamless nanotubes, but rather hemi-tubes. As shown in Figure 1, the silver tubular networks are composed of rolled silver nanosheets. We have also synthesized analogous silver nano-assemblies by use of other carboxylic acids such as capric acid, palmitic acid, and so on. The morphologies of the assemblies were quite different from each other, in particular the size of the assembled nanoparticles were different. The synthetic procedures for the silver nano-assemblies shown in Figure 4 were performed as follows: AgNO_3 (0.2 M, 144 μL) aqueous solutions and NaBH_4 (0.2 M, 144 μL) aqueous solutions were added to two different vessels both containing carboxylic acid/MMA (5 mL, 0.04 M) solutions; all other conditions were the same as those adopted in the lauric acid synthesis method mentioned above. As shown in Figure 4, most of the silver particles fabricated in the capric acid/MMA solution had a diameter of $3.0 \pm 1.0 \text{ nm}$, which is quite close to the diameter of the silver nanoparticles synthesized in the presence of lauric acid. This may be because there is no big difference in the chain length between lauric acid and capric acid, so they provide similar steric effects. However, the morphology of the resultant silver nano-assemblies formed in the capric acid/MMA solution were not networks. However, the diameters of the assembled silver nanoparticles obtained in the palmitic acid/MMA solution were much smaller than those created from the capric acid solution, being generally less than 2 nm; however, their self-assembly morphology was also branched, and similar to the networks generated with lauric acid. It has also been reported that the assembled silver nanoparticles obtained with the assistance of octanoic acid had a mean diameter of not less than 7 nm, and were therefore much larger than the particles we obtained in our research.^[15] We also discovered that no silver nano-assem-

blies could be obtained in the presence of *n*-hexanoic acid. Carboxylic acids with long carbon chains could provide strong protection for the silver nanoparticles, and therefore small particles would be obtained with the assistance of such carboxylic acids. If the carbon chain was short enough insufficient steric repulsion would be provided and no silver nano-assembly would be fabricated.

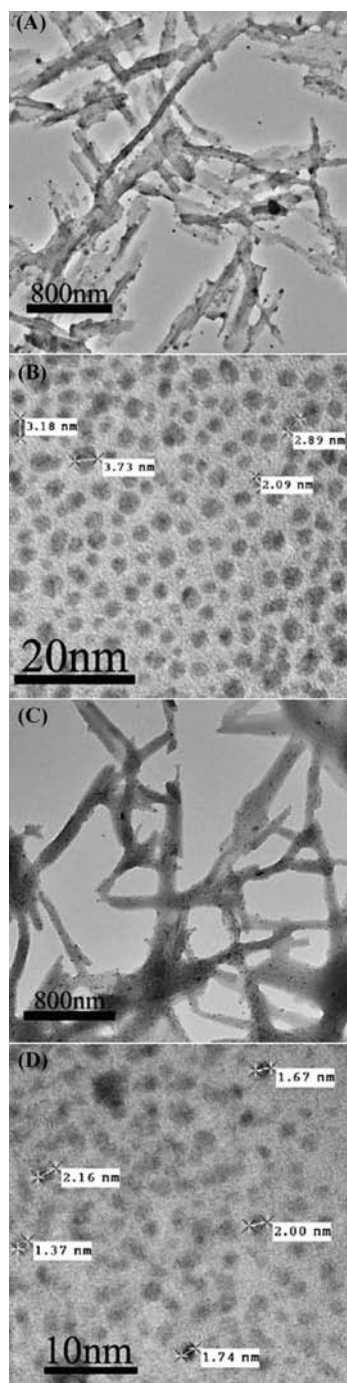


Figure 4. TEM and HRTEM images of the silver nano-assemblies synthesized in the presence of different carboxylic acids following a typical procedure. (A) and (B): 0.04 M capric acid/MMA solution, $W = 40$; (C) and (D): 0.04 M palmitic acid/MMA solution, $W = 40$.

From the experimental results reported herein, it can be concluded that the size of the assembled nanoparticles does not change significantly with changes in the concentration of AgNO_3 in the reaction solution. Therefore, it is impossible for each micelle to form a single silver nanoparticle; otherwise different precursor concentrations would result in the diameters of the assembled particles being different. In addition, the size of the resulting reverse micelles had been tracked by dynamic light scattering (DLS) measurements. As shown in Figure 5, the reverse micellar solution prepared from mixing aqueous NaBH_4 (0.2 M, 144 μL) with lauric acid/MMA (0.4 M, 5 mL) solution was more stable after 20 min sonication than the solution prepared from mixing aqueous AgNO_3 (0.2 M, 144 μL) with lauric acid/MMA (0.4 M, 5 mL) solution. The reverse micelles involving NaBH_4 would have relatively small diameters ranging from 350–850 nm during the first 18 min after 20 min of sonication. However, the reverse micellar solution involving AgNO_3 was unstable and the micellar diameter would change sharply from 1454–2516 nm 4 min after sonication.

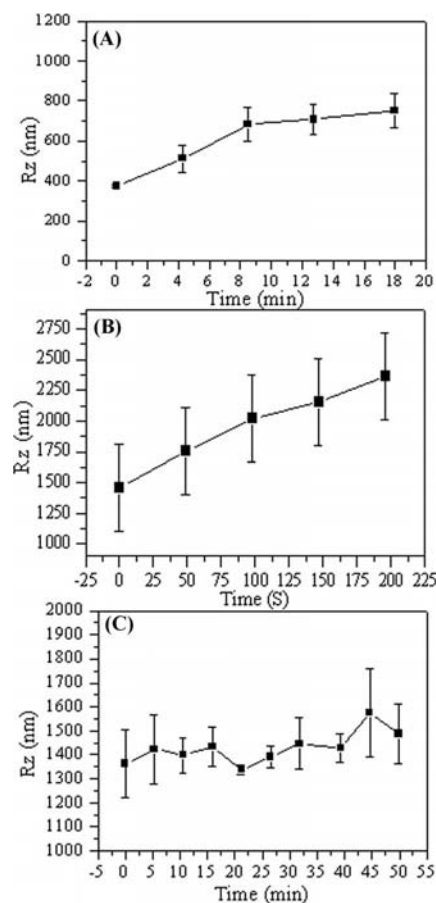
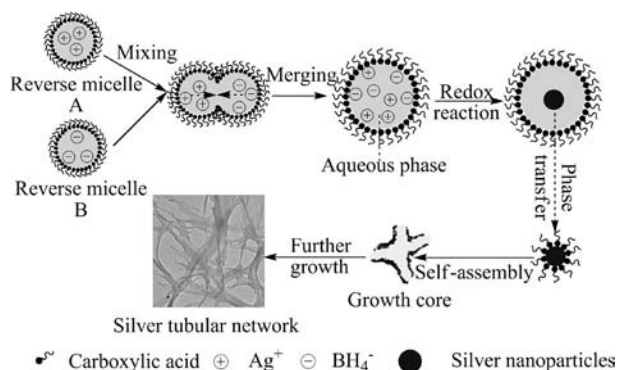


Figure 5. Hydrodynamic radius changes for different reverse micelles measured by DLS: (A) Reverse micellar solution prepared by mixing aqueous NaBH_4 (0.2 M, 144 μL) with lauric acid/MMA (0.4 M, 5 mL) solution after 20 min sonication; (B) reverse micellar solution prepared by mixing aqueous AgNO_3 (0.2 M, 144 μL) with lauric acid/MMA (0.4 M, 5 mL) solution after 20 min sonication; (C) reverse micellar solution prepared by mixing solutions A with B together. The error bars were plotted based on the standard deviation.

The diameter will continue to increase further after that time. It has been reported that NaBH_4 can be used as a methyl methacrylate stabilizer, and cannot reduce the carbonyl group in a carboxylic acid or ester species.^[29] Why the reverse micelles involving NaBH_4 are much more stable than those involving AgNO_3 is still unknown, and the detailed mechanism involved needs to be explored further. The whole solution involved in the assembly process was monitored by DLS and the results are shown in Figure 5. The reaction between NaBH_4 and AgNO_3 was very fast and the color of the solution changed within a few seconds after their reverse micellar solutions were mixed together. The mixed reverse micellar solution contained micelles that had relatively large diameters, with the average diameter fluctuating near 1450 nm during the course of the testing process. However, no peak approximating to the diameter of assembled nanoparticles was observed, this might be because the intense signal from the large micelles obscured that from the tiny nanoparticles.

As shown in Scheme 2, when the micellar solutions of the NaBH_4 and AgNO_3 were mixed together, different micelles collided with each other. After the reaction, the newly formed silver nanoparticles overcame environmental resistance to move into the organic phase as soon as they reached a critical size. The environmental resistance for small particles entering the organic phase might be interfacial tension, the surfactant resistance in the interface, repulsion due to the hydrophilicity of the particle surface, and so on.^[30] Therefore the size of the nanoparticles is determined predominantly by the resistance from the carboxylic acid at the interface, because carboxylic acids can change not only the interfacial tension, but also the surface hydrophilicity and steric repulsion of silver nanoparticles. Then the lauric acid stabilized nanoparticles further self-assemble into the nano-assembly in the organic phase due to the hydrophobicity of the adsorbed surfactant. It is believed that the interaction of the hydrophobic part of the surfactant with the solvent drives this nanoscale self-assembly process. Initially, the synthetic silver nanoparticles congregate to form the growth core in the organic phase. Several branches then grow out from this organic core, and these branches then grow longer through the continuous self-assembly of the



Scheme 2. Schematic illustration of the fabrication of silver nanotubular networks by the reverse micellar method.

silver nanoparticles. Despite changes in size, the branches formed early in the process can outgrow new branches formed later. The continuously generated silver nanoparticles epitaxially self-assemble onto the tip and outer surface of the branched nano-assembly layer by layer. As long as the appropriate steric repulsion is provided by lauric acid, a tubular silver network with both uniform structure and dense branches will be fabricated.

Conclusions

In summary, we have successfully fabricated a novel nanotubular network from a reverse micellar solution. It has been demonstrated that such supramolecular structures were formed by the self-assembly of silver nanoparticles with diameters of 3 ± 1 nm. In addition, densely branched networks comprising rolled silver nanosheets were fabricated with the assistance of lauric acid, especially when $W = 40$. Under other conditions, tubular silver networks with nonuniform structures or few branches were generated. The network morphology is favorable for the formation of continuous conductive networks in coatings, which makes the silver tubular networks excellent and promising conductive fillers, and the nanotubular networks self-assembled from small silver nanoparticles would be promising for showing significant surface-enhanced Raman scattering (SERS) effects. Therefore the fabrication of such silver nanotubular networks is meaningful and significant.

Experimental Section

Chemicals and Materials: Analytical grade AgNO_3 (Shanghai Reagent Factory, China), and MMA (Shanghai Chemical Reagent Purchase and Supply Wulian Chemical Factory, China) were used in this study. NaBH_4 , lauric acid, capric acid and cetylic acid were bought from Sinopharm Chemical Reagent Co. Ltd., China, and used as received.

Preparation of Silver Nanotubular Networks: The reverse micellar solutions containing AgNO_3 , NaBH_4 , MMA, surfactant (lauric acid), H_2O were used to synthesize the silver nanotubular networks. In a standard preparation, an aqueous solution of AgNO_3 (0.2 M, 144 μL) was added to a lauric acid/MMA solution (0.04 M, 5 mL) in a vessel with magnetic stirring. In a separate vessel under the same conditions an aqueous solution of NaBH_4 (0.2 M, 144 μL) was added to a lauric acid/MMA mixture (0.04 M, 5 mL). Then the oily mixtures from the different vessels were sonicated for 20 min to form the micellar solutions, and then the reverse micellar solution containing NaBH_4 was added to the vessel containing the AgNO_3 reverse micellar solution with vigorous stirring. The solution was then maintained at room temperature for 1 h. After completion of the reaction, the silver nano-assembly was separated from the reverse micellar solution by centrifugation and then washed with water. Then the surfactant was removed from the product by centrifugation and washing with ethanol. The centrifugation was carried out in an Anke TDL80-2B centrifuge at a rotating speed of 3000 rpm. The purified silver nano-assemblies were dispersed in ethanol to enable further characterization.

Characterization: TEM images were obtained with a Philips HR-TEM CM200 instrument, and the samples were prepared by drop-

ping a purified ethanol solution of the samples onto a copper grid. FT-IR spectra were recorded on a Thermo Nicolet 5700 infrared spectrophotometer, and the silver nano-assemblies and lauric acid, which were dispersed in ethanol, were dropped onto a KBr wafer. The SEM images and energy dispersive X-ray analyses were recorded with a FEI SIRION instrument. Before recording the SEM images the sample dispersion was dropped onto a silicon wafer to form a thin film, and after drying, the prefabricated sample was treated with gold spray to improve the conductivity. The gold spraying was performed on an E-1030 ion sputter. Particle size analysis was performed by dynamics light scattering on a Malvern Zetasizer 3000HSA Laser Nanometer Particle Size Analyzer. The wavelength of the laser source was 633 nm. The refractive index (RI) and viscosity of MMA were used to approximate the dispersant RI and solution viscosity in the particle sizing analysis, and the RI of water was set as the Real Refractive Index in the testing software. Due to the micellar instability, the particle size analysis of the reverse micellar solution involving AgNO₃ was conducted five times with each run comprising only one cycle lasting 40 s. The other samples were also run five times with each run comprising 10 cycles each of which lasted 3 min.

Acknowledgments

Financial support from the Ministry of Science and Technology (863 project) is gratefully acknowledged

- [1] W. Zeng, S. T. Tan, *Polym. Compos.* **2006**, 27, 24–29.
- [2] G. Jiang, M. Gilbert, D. J. Hitt, G. D. Wilcox, K. Balasubramanian, *Composites: Part A* **2002**, 33, 745–751.
- [3] M. J. Yim, Y. Li, K. S. Moon, C. P. Wong, *J. Electron. Mater.* **2010**, 36, 1341–1347.
- [4] Y. S. Lin, S. S. Chiu, *J. Adhes. Sci. Technol.* **2008**, 22, 1673–1697.
- [5] E. Sancaktar, N. Dilsiz, *J. Adhes. Sci. Technol.* **1999**, 13, 763–771.
- [6] H. Wu, X. Wu, *Acta Materialiae Compositae Sinica* **2006**, 23, 24–28.
- [7] Z. Zhang, L. Shi, *J. Functional Mater.* **2008**, 39, 337–340.
- [8] H. P. Wu, J. F. Liu, X. J. Wu, M. Y. Ge, Y. W. Wang, G. Q. Zhang, J. Z. Jiang, *Int. J. Adhes. Adhes.* **2006**, 26, 617–621.
- [9] C. Chen, L. Wang, R. L. Li, G. H. Jiang, H. J. Yu, T. Chen, *J. Mater. Sci.* **2007**, 42, 3172–3176.
- [10] D. P. Chen, X. L. Qiao, X. L. Qiu, J. G. Chen, *J. Mater. Science* **2009**, 44, 1076–1081.
- [11] Y. Sun, B. Gates, B. Mayers, Y. Xia, *Nano Lett.* **2002**, 2, 165–168.
- [12] R. Sharabani, S. Reuveni, G. Noy, E. Shapira, S. Sadeh, Y. Selzer, *Nano Lett.* **2008**, 8, 1169–1173.
- [13] C. Chen, L. Wang, G. H. Jiang, J. F. Zhou, X. Chen, H. J. Yu, Q. Yang, *Nanotechnology* **2006**, 17, 3933–3938.
- [14] K. E. Korte, S. E. Skrabalak, Y. Xia, *J. Mater. Chem.* **2008**, 18, 437–441.
- [15] J. H. Liu, C. Y. Tsai, Y. H. Chiu, F. M. Hsieh, *Nanotechnology* **2009**, 20, 035301–035310.
- [16] L. A. Peyser, A. E. Vinson, A. P. Bartko, R. M. Dickson, *Science* **2001**, 291, 103–106.
- [17] A. Maali, T. Cardinal, M. Treguer-Delapierre, *Phys. E* **2003**, 17, 559–560.
- [18] J. Selva, S. E. Martinez, D. Buceta, M. Rodriguez-Vazquez, M. C. Blanco, M. A. Lopez-Quintela, G. Egea, *J. Am. Chem. Soc.* **2010**, 132, 6947–6954.
- [19] L. Zhou, C. G. Freyschlag, B. Xu, C. M. Friend, R. J. Madix, *Chem. Commun.* **2010**, 46, 704–706.
- [20] Y. Lu, G. L. Liu, L. P. Lee, *Nano Lett.* **2005**, 5, 5–9.
- [21] H. H. Wang, C. Y. Liu, S. B. Wu, N. W. Liu, C. Y. Peng, T. H. Chan, C. F. Hsu, J. K. Wang, Y. L. Wang, *Adv. Mater.* **2006**, 18, 491–495.
- [22] K. Nomiya, S. Takahashi, R. Noguchi, S. Nemoto, T. Takayama, M. Odas, *Inorg. Chem.* **2000**, 39, 3301–3311.
- [23] Y. Sun, Y. Xia, *Adv. Mater.* **2002**, 14, 833–837.
- [24] Y. Gao, P. Jiang, D. F. Liu, H. J. Yuan, X. Q. Yan, Z. P. Zhou, J. X. Wang, L. Song, L. F. Liu, W. Y. Zhou, G. Wang, C. Y. Wang, S. S. Xie, J. M. Zhang, A. Y. Shen, *J. Phys. Chem. B* **2004**, 108, 12877–12881.
- [25] W. Wang, S. Efrima, O. Regev, *Langmuir* **1998**, 14, 602–610.
- [26] Y. Wang, H. Xu, X. Zhang, *Adv. Mater.* **2009**, 21, 2849–2864.
- [27] K. J. M. Bishop, C. E. Wilmer, S. Soh, B. A. Grzybowski, *Small* **2009**, 5, 1600–1630.
- [28] J. N. Israelachvili, H. Wennerstroem, *J. Phys. Chem.* **1992**, 96, 520–531.
- [29] S. L. Snyder, *J. Appl. Polym. Sci.* **1979**, 24, 2237–2241.
- [30] R. N. Wenzel, *Ind. Eng. Chem.* **1936**, 28, 988–994.

Received: September 8, 2010

Published Online: February 17, 2011